



Electrodeposition of Platinum Nanoparticles on Polyaniline Modified Electrode and its Electrocatalytic Activity towards the Oxidation of Methanol

ALI PARSA*, SEYED AMIR MIRSHAFIEYAN, AZADEH SHAKERI
and SARA AMANZADEH-SALOUT

Department of Chemistry, College of Science, Yadegar -e- Imam Khomeini (RAH)
Shahre-rey Branch, Islamic Azad University, Tehran, Iran.

*Corresponding author E-mail: aliparsa@iaus.ac.ir

<http://dx.doi.org/10.13005/ojc/320410>

(Received: June 10, 2016; Accepted: July 17, 2016)

ABSTRACT

In this research, we reported the electrosynthesis of platinum nanoparticles on Polyaniline (PAni) modified electrode. The modified electrodes were prepared by incorporation of aniline and platinum salt [H_2 (PtCl₆), 6H₂O] in phosphoric acid medium with KCl solution on composite graphite (CG) surface via cyclic voltammetry (CV) method. The synthesized platinum nanoparticles were characterized by using scanning electronic microscopy (SEM) and energy dispersive X-ray spectroscopy (EDX). The electro oxidation of methanol was investigated at the surface of these modified electrodes using CV method. It was found that methanol was oxidized with platinum embedded on the surface of PAni modified electrodes during the anodic potential sweep. Moreover, several impact factors such as scan rate, potential and concentration of methanol were studied on the oxidation of methanol toward electrosynthesized electrodes.

Keyword: Electrodeposition; Electrocatalytic oxidation;
Platinum nanoparticle; Methanol; Polyaniline.

INTRODUCTION

More demand for applying conducting polymers has led to improve the technology of synthesis them as the materials with wide applications. A thin film of conducting polymer on the electrode may improve the electro-catalytic activity and so, it may be increased¹⁻⁶. The conducting polymers can also cause the easier charge transfer

during the electrochemical oxidation of alcohols on Pt surface⁷. PAni is one of the most extensively studied conducting polymers due to its easy synthesis, high conductivity, environmental stability and reversible redox catalytic properties⁸⁻¹⁵. The metal nanoparticles, such as Pt, on PAni modified electrode show catalytic properties for organic fuel oxidation¹⁶⁻¹⁹. Fuel cells are known as one of the best electrical power to obtain the electrical

energy from the combustion of hydrogen or organic compounds, than other sources²⁰⁻²². Up to know, Pt is a good catalyst for methanol oxidation, but, because of the poisoning by CO absorption it has low stability. Some research was accomplished to study of CO adsorption and Methanol oxidation on Pt electrodes modified by electrodeposition of PANi film²³⁻²⁵. In those researches PANi is specified as the context for electro oxidation of hydrogen and methanol by applying the metal catalysts because of increasing the catalytic area for incorporating the metallic particles²⁶⁻²⁸. The PANi/Pt nanoparticles electrode has exhibited excellent catalytic activity for methanol oxidation in various mediums^{27, 29-32}. In this research the Pt nanoparticles were electrodeposited on PANi/CG electrodes with the noble condition of synthesis (during and after the formation of PANi films in phosphoric acid medium and KCl supporting electrolyte), and the electrocatalytic oxidation of methanol on modified electrodes was investigated with the purpose of improving highly active sites of electrodes.

MATERIALS AND METHODS

Aniline (Merck, Germany) was distilled under low pressure in the atmosphere and liquid nitrogen at a temperature of 5 °C until color was maintained. Methanol (MeOH) (BDH Chemicals, UK) was also in pure form. The hexachloro platinumic (IV) acid hexahydrate [$H_2 (PtCl_6) 6H_2O$] (Sigma Chemicals, USA), potassium chloride (KCl) (Fluka

Chemicals, Switzerland) and phosphoric acid (H_3PO_4) (Sigma Chemicals, USA) were used without purification.

Equipment

The electrochemical analysis for the synthesis and characterization of nano-composite electrodes was carried out by a potentiostat/galvanostat compactstat (Ivium Technologies, Netherlands). SEM, model VEGA Corporation (TESCAN) Czechoslovakia equipped with EDX detector has been used to investigate the morphology and size of the Pt nanoparticles on PANi modified electrodes. The composite 2B pencil graphite (CG) (o.d. 1.8 mm) (Staedtler Lumograph, Germany) was used as working electrode against pseudo Ag/AgCl reference electrode.

Procedure

The electrochemical synthesis of PANi was done by 50 mM aniline in 10 mL of 1 M H_3PO_4 and 0.5 M KCl as a supporting electrolyte, on the working electrode (CG) by sweeping the potential continuously between -0.2 V to +1.00 V vs. Ag/AgCl with a scan rate of 100 mVs⁻¹. Also the Pt particles were incorporated by electrochemical deposition from a solution containing 0.01% wt. [$H_2 (PtCl_6) 6H_2O$] in 1 M H_3PO_4 on working electrode.

RESULTS AND DISCUSSIONS

Electrodeposition

Electrodeposition of PANi on CG (PANi/CG)

The cyclic voltammograms (CVs) for the deposition of PANi on CG electrode from the 50 mM

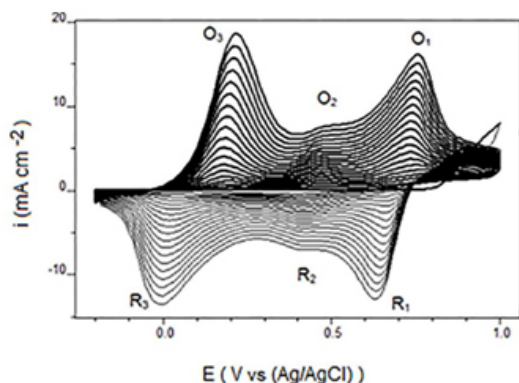


Fig. 1: CVs of 50 mM Ani in 1 M H_3PO_4 containing 0.5 M KCl on CG electrode. The scan rate is 100 mVs⁻¹

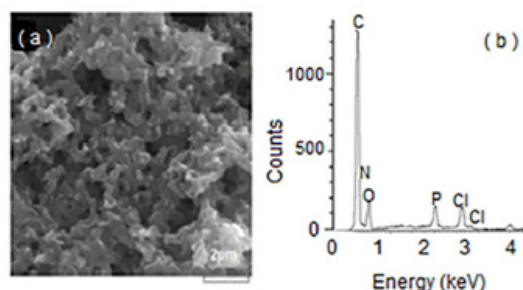


Fig. 2: SEM and EDX analysis of electrosynthesized PANi in 1 M H_3PO_4 containing 0.5 M KCl on CG electrode, (a) SEM (b) EDX

aniline in aqueous medium of 10 mL of 1 M H_3PO_4 and 0.5 M KCl is shown in Fig.1. The three pairs of redox peaks are the result of aniline configuration conversions observed in the potential range of -0.2 V to +1.0 V. The first pair of redox peaks denoted as O_3/R_3 corresponds to the interconversion of the completely PANi reduced form, leucoemeraldine (LE) state, to the half-oxidized emeraldine base (EB) state. The second pair of redox peaks denoted as O_1/R_1 is due to oxidation of EB to the completely oxidized pernigraniline (PN) state and vice-versa. The O_2/R_2 peaks are attributed to oxidation of segments of PANi chain to benzoquinone (Bq) species, whose peak potentials are very close to one another and tend to disappear after several successive scans³³. Fig. 2a shows the surface morphology of PANi film on CG electrode. In the EDX analysis (Fig. 2b) the existence of phosphate ions is shown. This confirms that the doping of aniline with phosphate during polymerization has occurred on the surface of graphite electrode.

Electrodeposition of Pt nanoparticles on PANi/CG electrode (*NPPt/PANI/CG*)

The Platinum nanoparticles were incorporated by electrochemical deposition on PANi/CG electrode from $\text{H}_2\text{PtCl}_6 \cdot 6\text{H}_2\text{O}$ solution (0.01% w/w) containing 1 M H_3PO_4 and 0.5 M KCl (Fig. 3). The CVs reveal one pair of redox peaks that represent the electrodeposition of Pt(IV) to metallic Pt on the surface of PANi/CG film in accordance with reaction (1)²⁷.

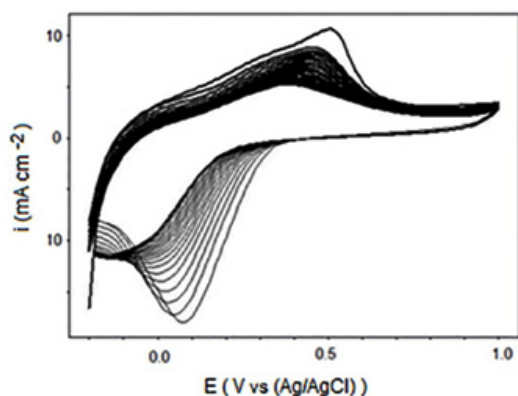


Fig. 3: The cyclic voltammogram obtained during electrodeposition of Pt nanoparticles on (PANi/CG) electrode in 1 M H_3PO_4 containing 0.5 M KCl. The scan rate is 100 mVs^{-1} .



Fig. 4a shows a fully homogenized surface of electrode. This confirms that distribution of Pt on PANi film is completely uniform. Also it shows the Pt nanoparticles on the PANi/CG electrode (Fig. 4b). EDX spectrum confirms the uniform presence of Pt nanoparticles on the surface of electrode (Fig. 4c).

Simultaneous electrodeposition of Pt and PANi on CG (*Pt-PANI/CG*)

The platinum nanoparticles and PANi were, simultaneously, electrodeposited on CG from a solution of $\text{H}_2\text{PtCl}_6 \cdot 6\text{H}_2\text{O}$ (0.01% w/w), 50 mM aniline, 1 M H_3PO_4 and 0.5 M KCl. As shown in Fig. 5 the CVs have two redox peaks. In this case, it is seen that PANi is in the conducting emeraldine salt (ES) form which undergoes the oxidation to the PN form, providing electrons for the reduction of PtCl_6^{-2} to metallic Pt.

Fig. 6a and b shows that, spherical Pt is in context with PANi after the simultaneous deposition. As compared to *NPPt/PANI/CG*, the distribution and dispersal is less. The absence of Pt in depth of 4 microns was confirmed by EDX analysis (Fig. 6c). As is evident the nanostructure can be changed with monomer displacement, i.e., the conductivity of PANi

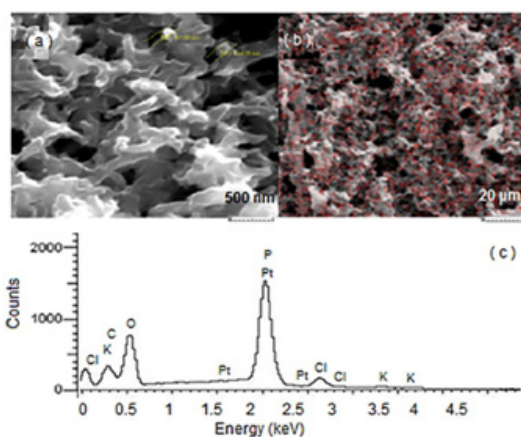


Fig. 4. SEM and EDX analysis of Pt nanoparticles on modified (*NPPt/PANI/CG*) electrode in 1 M H_3PO_4 containing 0.5 M KCl. (a) and (b) SEM image of (*NPPt/PANI/CG*) electrode at different magnifications (c) EDX analysis of Pt nanoparticles on (PANi/CG) electrode

can play important role in doping and polymerizing of PANi with platinum ions. This result may also be attributed to the higher conductivity and faster charge transfer of PANi film in the intermediate oxidation state. It must be pointed out that the catalytic current is greatly in-creased with increase in the amount of deposited Pt ³⁴.

Electrocatalytic oxidation of methanol

Fig. 7a and b shows the CVs of Pt-PANI/CG and *NPPt*/PANI/CG electrodes in 1 M H₃PO₄

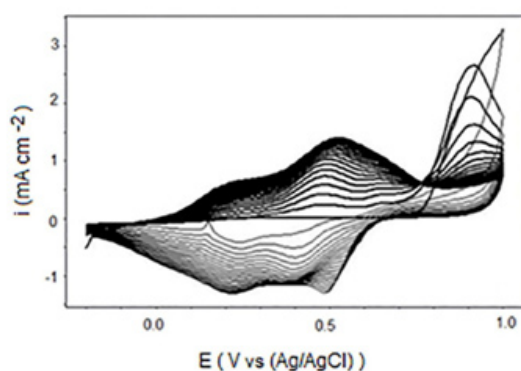


Fig. 5: Cyclic voltammogram of Simultaneous electro-synthesis of Pt nanoparticles and PANi at on CG electrode in a solution of 1 M H₃PO₄ containing 0.5 M KCl, H₂PtCl₆·6H₂O (0.01% w/w) and 50 mM aniline. The scan rate is 100 mVs⁻¹

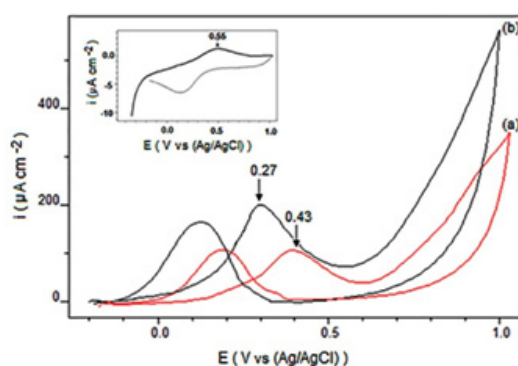


Fig. 7: CVs of, (a) (Pt-PANI/CG) and (b), (*NPPt*/PANI/CG) electrodes in 1 M H₃PO₄ solution containing 0.5 M methanol at scan rate of 100 mVs⁻¹. Inset: CV of unmodified CG electrode in 1 M H₃PO₄ solution and 0.5 M methanol at scan rate of 100 mVs⁻¹

containing 0.5 M methanol at a scan rate of 100 mVs⁻¹, respectively. The methanol oxidations of Pt-PANI/CG (E_{pa} = 0.43V) and *NPPt*/PANI/CG in (E_{pa} = 0.27V) indicate that *NPPt*/PANI/CG has a relatively superior electrocatalytic performance. The

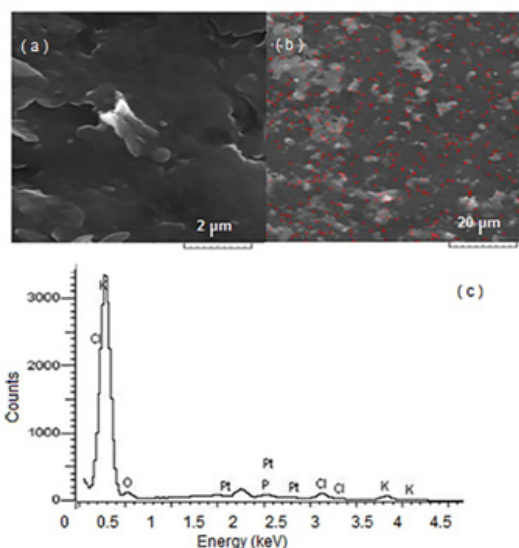


Fig. 6: SEM and EDX analysis of Pt nanoparticles on modified (Pt-PANI/CG) electrode in 1 M H₃PO₄ containing 0.5 M KCl. (a) and (b) SEM image of (Pt-PANI/CG) electrode at different magnifications (c) EDX analysis of (Pt-PANI/CG) electrode

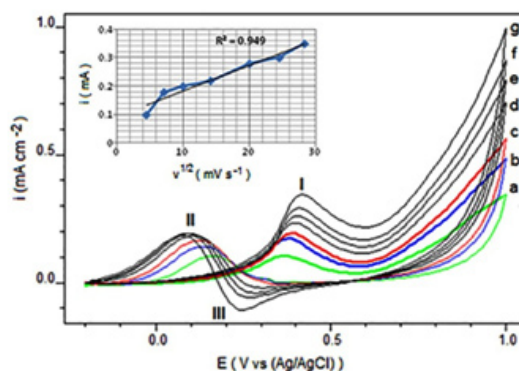
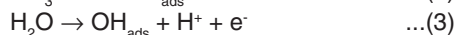


Fig. 8: CVs of (*NPPt*/PANI/CG) prepared in 1 M H₃PO₄ and 0.5 M methanol at different scan rates (a) 20, (b) 60, (c) 100, (d) 200, (e) 400, (f) 600, (g) 800 mVs⁻¹ in the potential range of -0.2 V to 1.0 V. Inset the calibration plot of current vs. square root of scan rate

Table 1: CVs data of (NPPt/PAni/CG) and (Pt-PAni/CG) electrode

Electrode	Charge of H ₂ absorption	max anodic peak current (I _{pa})
(NPPt/PAni/CG)	3.14 mC /cm ²	19.32 mA /cm ²
(Pt-PAni/CG)	2.07 mC /cm ²	10.09 mA /cm ²

electrochemical oxidation of methanol on Pt surface occurs in two steps³⁵. The first step is methanol dehydrogenation in which, methanol is oxidized to become adsorbed CO_{ads} species. The second step is the removal of CO_{ads} which proceeded via adsorbed OH_{ads} to produce CO₂. The adsorbed OH_{ads} is produced from water dissociation process on Pt catalyst sites. The overall processes are summarized in reactions (below):



It is known that the integrated intensity of hydrogen absorption represents the number of Pt sites that are available for hydrogen adsorption and desorption²⁵. To calculate the charge required for hydrogen adsorption on the electrode surfaces, we assume that the double-layer charging current is constant over the whole potential range³⁶. The charge required for hydrogen adsorption on the NPPt/PAni/CG surface is 3.14 mC cm⁻² which is 1.5 times larger than that required for hydrogen adsorption on the Pt-PAni/CG surface (2.07 mC cm⁻²), (Table 1). Comparing the CV results of NPPt/PAni/CG with Pt-PAni/CG electrodes, have indicated a significantly higher oxidation current toward methanol oxidation for the NPPt/PAni/CG electrode. For instance, in Table 1, the maximum anodic peak current densities (I_{pa}) for NPPt/PAni/CG and Pt-PAni/CG electrodes are 19.32 mA cm⁻² and 10.09 mA cm⁻², respectively. A high surface area for Pt particles in NPPt/PAni/CG is anticipated due to the uniform distribution of Pt particles into PAni which can twist up to form a spatial 3D dimensional matrix. In addition to this, the -CO₂H groups in NPPt/PAni/CG may act as a stabilizer for Pt particles, preventing their aggregation. The PAni/CG matrix acts as a good bed for the deposition of Pt particles, and increases the density of the active sites on the electrode surface.

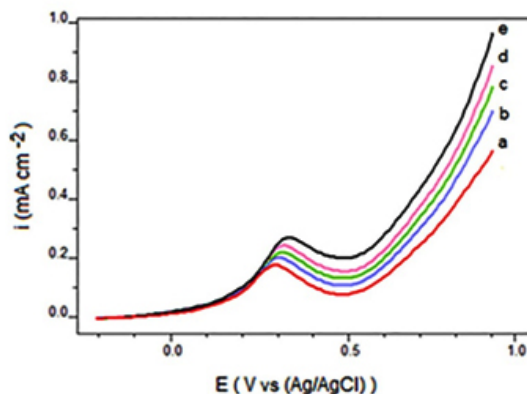


Fig. 9: LSVs of (NPPt/PAni/CG) prepared in 1 M H₃PO₄ with different concentration of methanol (a) 0.5 M, (b) 1 M, (c) 2 M, (d) 3 M, (e) 4 M in potential range of -0.2 V to +1.0 V

Effect of scan rate on the oxidation of methanol

Figure 8a to g shows the CVs of NPPt/PAni/CG in 1M H₃PO₄ containing 0.5 M methanol at the various scan rates and in the potential range of -0.2V to 1.0 V. This indicates that, increasing the scan rate has led to increase the I_{pa} and cause to improve the methanol oxidation. In the lower scan rates, i.e. less than 200 mVs⁻¹, two well define redox peaks are observed. The first I_{pa} is produced due to the oxidation of freshly chemisorbed species coming from methanol adsorption. The second I_{pa} is primarily associated with the removal of carbonaceous species not completely oxidized in forward scan rather than caused by freshly chemisorbed species. In the higher scan rates (more than 200 mVs⁻¹) there are three oxidation peaks, the second and third in the reverse scan is additional, which is due to a combination processes such as surface rearrangement and increase of the heterogeneous non-faradaic reaction rate^{37, 28, 38}. The plot of I_p vs. square root of scan rate (inset) is linear, which is indicates that the electrochemical process was under diffusion control

Effect of methanol concentration on electrocatalytic activity

Figure 9a to d shows the linear sweep voltammograms (LSVs) of NPPt/PAni/CG in 1 M H₃PO₄ containing different concentration of methanol at the potential range of -0.2 V to 1.0 V. A significant enhancement of methanol oxidation has been

observed at high concentration of methanol as shown by the increase of the oxidation peak current (I_{pa}).

CONCLUSION

The platinum nanoparticles were successfully electrodeposited onto the surface of PANi/CG electrodes. The NPPt/PAni/CG electrode appeared to have well distribution and dispersal of Pt nanoparticles on the PANi film. The NPPt/PAni/CG electrode exhibited electrocatalytic activity toward methanol oxidation with a higher current density and

at lower onset potential. In view of results, the higher concentrations of methanol and higher scan rates of potential have also enhanced the methanol oxidation. According to the extensive studies in this filed, still further research can complement and corroborate these results.

ACKNOWLEDGEMENTS

This work is supported by the Islamic Azad University, Yadegar -e- Imam Khomeini (RAH) Shahre-rey Branch, Tehran, Iran for Research University (RU) grant -1395/1742:90/07/27

REFERENCES

1. Su, N. *Nanoscale Res. Lett.* **2015**, *10*, 1-9 .
2. Campbell, D. K. *Synth. Met.* **2001**, *125*, 117-128 .
3. Macdiarmid, A. G. *Synth. Met.* **1987**, *21*, 79-83 .
4. Wallace, G. G.; Smyth, M.; Zhao, H. *TrAC, Trends Anal. Chem.* **1999**, *18*, 245-251 .
5. Lange, U.; Roznyatovskaya, N. V.; Mirsky, V. M. *Anal. Chim. Acta.* **2008**, *614*, 1-26 .
6. Morteza, E.; Roya, D. *Orient. J. Chem.* **2015**, *31*, 1185-1189 .
7. Serra, D.; McElwee-White, L. *Inorg. Chim. Acta.* **2008**, *361*, 3237-3246 .
8. MacDiarmid, A.; Chiang, J.; Richter, A.; Epstein, A. *Synth. Met.* **1987**, *18*, 285-290 .
9. MacDiarmid, A.; Yang, L.; Huang, W.; Humphrey, B. *Synth. Met.* **1987**, *18*, 393-398 .
10. Genies, E.; Boyle, A.; Lapkowski, M.; Tsintavis, C. *Synth. Met.* **1990**, *36*, 139-182 .
11. Luzny, W.; Banka, E.; Stochmal-Pomarzanska, E. *X-Ray Investigations of Polymer Structures.* **2000**, 47-50 .
12. Æiriæ-Marjanoviæ, G. *Synth. Met.* **2013**, *177*, 1-47 .
13. Kajornkavinkul, S.; Punrat, E.; Siangproh, W.; Rodthongkum, N.; Praphairaksit, N.; Chailapakul, O. *Talanta.* **2016**, *148*, 655-660 .
14. Ameen, S.; Shaheerakhtar, M. *Orient. J. Chem.* **2013**, *29*, 837-860 .
15. Udmale, V.; Mishr, D.; Gadhave, R.; Pinjare, D.; Yamgar, R. *Orient. J. Chem.* **2013**, *29*, 927-936 .
16. Han, Y.-K.; Chang, M.-Y.; Ho, K.-S.; Hsieh, T.-H.; Tsai, J.-L.; Huang, P.-C. *Sol. Energy Mater. Sol. Cells.* **2014**, *128*, 198-203 .
17. Farghali, A.; Moussa, M.; Khedr, M. *J. Alloys Compd.* **2010**, *499*, 98-103 .
18. Abaci, S.; Nessark, B.; Boukherroub, R.; Lmimouni, K. *Thin Solid Films.* **2011**, *519*, 3596-3602 .
19. Lemos, H. G.; Santos, S. F.; Venancio, E. C. *Synth. Met.* **2015**, *203*, 22-30 .
20. Andújar, J.; Segura, F. *Renew Sust Energ Rev.* **2009**, *13*, 2309-2322 .
21. Behling, N. H. *Fuel Cells.* **2013**, 423-600 .
22. Sharma, R.; Kar, K. K. *Electrochim. Acta.* **2015**, *156*, 199-206 .
23. Wang, Z.; Gao, G.; Zhu, H.; Sun, Z.; Liu, H.; Zhao, X. *Int. J. Hydrogen Energy.* **2009**, *34*, 9334-9340 .
24. Yan, R.; Jin, B. *Electrochim. Acta.* **2014**, *115*, 449-453 .
25. Gyenge, E. *PEM Fuel Cell Electrocatalysts and Catalyst Layers.* **2008**, 165-287 .
26. Lei, X.; Guo, X.; Zhang, L.; Wang, Y.; Su, Z. *J. Appl. Polym. Sci.* **2007**, *103*, 140-147 .
27. Sugano, Y.; Yoshikawa, H.; Saito, M.; Tamiya, E. *Electrochim. Acta.* **2011**, *56*, 9875-9882 .
28. Stejskal, J.; Sapurina, I.; Trchová, M. *Prog. Polym. Sci.* **2010**, *35*, 1420-1481 .
29. O'Mullane, A. P.; Dale, S. E.; Day, T. M.; Wilson, N. R.; Macpherson, J. V.; Unwin, P. R. *J. Solid State Electrochem.* **2006**, *10*, 792-807 .
30. Hong, T.-Z.; Xue, Q.; Yang, Z.-Y.; Dong, Y.-P.

- J. Power Sources*. **2016**, *303*, 109-117 .
31. Wang, M.; Song, X.; Yang, Q.; Hua, H.; Dai, S.; Hu, C.; Wei, D. *J. Power Sources*. **2015**, *273*, 624-630 .
32. Wang, Z.; Shi, G.; Zhang, F.; Xia, J.; Gui, R.; Yang, M.; Bi, S.; Xia, L.; Li, Y.; Xia, L.; Xia, Y. *Electrochim. Acta*. **2015**, *160*, 288-295 .
33. Parsa, A.; Ab Ghani, S. *Polymer*. **2008**, *49*, 3702-3708 .
34. Cai, L.; Chen, H. *J. Appl. Electrochem*. **1998**, *28*, 161-166 .
35. Tripkoviæ, A. V.; Popoviæ, K. D.; Loviæ, J.; Jovanoviæ, V.; Kowal, A. *J. Electroanal. Chem*. **2004**, *572*, 119-128 .
36. Wu, T.-Y.; Li, W.-B.; Kuo, C.-W.; Chou, C.-F.; Liao, J.-W.; Chen, H.-R.; Tseng, C.-G. *International Journal of Electrochemical Science*. **2013**, 10720-10732 .
37. Singh, R.; Awasthi, R.; Tiwari, S. *Open Catal. J*. **2010**, *3*, 54-61 .
38. Prabakar, S. J. R.; Kim, Y.; Jeong, J.; Jeong, S.; Lah, M. S.; Pyo, M. *Electrochim. Acta*. **2016**, *188*, 472-479 .